

MRI of Cardiac Sarcoidosis: Basal and Subepicardial Localization of Myocardial Lesions and Their Effect on Left Ventricular Function

Azusa Ichinose¹
 Hiroki Otani²
 Minako Oikawa²
 Kei Takase¹
 Haruo Saito¹
 Hiroaki Shimokawa²
 Shoki Takahashi¹

OBJECTIVE. The objective of our study was to use MRI to analyze the topographic localization of myocardial lesions and their relationship to plasma brain natriuretic peptide (BNP) levels and several cardiac function parameters in patients with cardiac sarcoidosis.

MATERIALS AND METHODS. Delayed contrast-enhanced MRI was performed in 40 patients with sarcoidosis (11 cardiac, 29 extracardiac cases). Using a 29-segment model of the left ventricle (LV), the extent of myocardial hyperenhancement was visually scored (0 = no hyperenhancement, 1 = 1–25%, 2 = 26–50%, 3 = 51–75%, 4 = 76–100% hyperenhancement) and was compared with plasma BNP level and several parameters of cardiac function.

RESULTS. Ten of the 11 patients with cardiac sarcoidosis showed myocardial hyperenhancement, whereas none of the 29 patients without cardiac sarcoidosis did. In patients with cardiac sarcoidosis, hyperenhancement was significantly more extensive in basal short axis slices than in apical short axis slices ($p < 0.0005$). Myocardial hyperenhancement was significantly more frequent in subepicardial layers than in subendocardial layers. The global extent of myocardial hyperenhancement was significantly correlated with plasma BNP levels and the LV end-diastolic volume index and was negatively correlated with the LV ejection fraction.

CONCLUSION. In patients with cardiac sarcoidosis, myocardial lesions detected on delayed contrast-enhanced MRI were predominantly localized in the basal and subepicardial myocardium. The extent of myocardial lesions may be related to LV dysfunction and plasma BNP level in patients with cardiac sarcoidosis.

Keywords: delayed contrast enhancement, left ventricular function, MRI, myocardium, myocardial infarction, noncaseating granulomas, sarcoidosis

DOI:10.2214/AJR.07.3089

Received August 25, 2007; accepted after revision March 17, 2008.

¹Department of Radiology, Tohoku University Graduate School of Medicine, Seiryomachi, Aobaku, Sendai 980-8574, Japan. Address correspondence to A. Ichinose (azusa@rad.med.tohoku.ac.jp).

²Department of Cardiovascular Medicine, Tohoku University Graduate School of Medicine, Aobaku, Sendai, Japan.

AJR 2008; 191:862–869

0361–803X/08/1913–862

© American Roentgen Ray Society

Sarcoidosis is a multisystem disorder of unknown cause characterized by the infiltration of noncaseating granulomas. The overall prognosis for patients with sarcoidosis is good because there is usually no organ involvement and the disease is often self-limiting [1]. However, sarcoidosis with cardiac involvement can cause fatal ventricular tachyarrhythmias, conduction disturbances, and left ventricle (LV) dysfunction [2].

Although cardiac involvement in sarcoidosis has been reported to be clinically evident in fewer than 5% of patients with sarcoidosis [3], postmortem studies have revealed cardiac involvement in 20–27% of such patients in the United States [2]. In Japan, cardiac involvement is frequently present in up to 58% of patients with sarcoidosis at autopsy and is responsible for as many as 85% of the deaths from sarcoidosis [4]. Current diagnostic imaging techniques such as 2D echocardiography and SPECT myocardial

perfusion imaging have the disadvantages of low sensitivity or low specificity (or both) for diagnosing cardiac sarcoidosis [5, 6].

Delayed contrast-enhanced MRI with an inversion recovery sequence allows visualization of scar tissue in patients with myocardial infarction (MI) or hypertrophic cardiomyopathy [7–9]. Delayed contrast-enhanced MRI is also useful for evaluating and monitoring inflammatory heart disease [10]. Several reports have shown the usefulness of delayed contrast-enhanced MRI with an inversion recovery sequence in patients with cardiac sarcoidosis [11–13], but the topographic and intramural localization of myocardial lesions, shown as regions of hyperenhancement, is poorly understood. Furthermore, the association between the extent of hyperenhancement and LV global function has not been clarified.

In the present study, we examined whether delayed contrast-enhanced MRI is useful for determining the topographic and intramural

MRI of Cardiac Sarcoidosis

localization of myocardial lesions in patients with cardiac sarcoidosis. We also tested the hypothesis that the extent of myocardial lesions is correlated with LV enlargement, LV systolic dysfunction, and plasma concentrations of brain natriuretic peptide (BNP), all of which are useful prognostic markers in patients with heart failure [14, 15].

Materials and Methods

Patient Population

Written informed consent was obtained from every subject before commencing the study. The purpose and nature of this study were approved by the ethics committees of our institute.

We retrospectively studied 40 consecutive patients with systemic sarcoidosis who underwent MRI between June 2002 and May 2005. All patients were diagnosed with sarcoidosis on the basis of histologic evidence of noncaseating epithelioid granulomas with giant cells. Biopsies were obtained from lung ($n = 16$), lymph nodes ($n = 11$), skin ($n = 10$), muscle ($n = 2$), and bone ($n = 1$). The patients either had cardiac symptoms ($n = 16$) or were screened for cardiac involvement in the absence of cardiac symptoms ($n = 24$). All patients underwent standard 12-lead ECG, 24-hour Holter monitoring, and echocardiography.

According to the Japanese Ministry of Health and Welfare guidelines [16] (Appendix 1), 11 patients in the study were clinically diagnosed with cardiac sarcoidosis. Coronary angiography excluded coronary artery disease in all patients. Confirmation of cardiac sarcoidosis by endomyocardial biopsy was not obtained for any of the

patients. Plasma BNP level was measured in all 11 patients with cardiac sarcoidosis and in 22 of the 29 patients without cardiac sarcoidosis within 2 weeks of the MRI study. Plasma BNP levels were not measured in the seven remaining patients without cardiac sarcoidosis.

MRI Protocol

MRI was performed after the patients had been clinically stabilized after heart failure. ECG-gated MR images were obtained in all patients during breath-holding on a 1.5-T imager (Magnetom Vision, Siemens Medical Solutions) using a body array coil. To evaluate LV anatomy and function, cine MR images of the LV in one horizontal, one vertical long, and five short axis slices were obtained using a gradient-echo sequence (FLASH). Five short axis slices at 14-mm intervals were set from 1 cm below the level of the mitral valve insertion to the apex, roughly covering the entire LV. The acquisition parameters were TR/TE, 11.3/6.1; flip angle, 25°; field of view, 300 mm; 7 lines per segment; matrix, 182 × 256; and slice thickness, 5 mm.

Using the same slice levels as described, delayed contrast-enhanced MR images using inversion recovery turbo FLASH with a segmented inversion recovery gradient-echo pulse sequence [17] were acquired 15 minutes after the injection of gadopentetate dimeglumine (0.15 mmol/kg). The acquisition parameters were 7.5/3.4; flip angle, 15°; field of view, 300 mm; 33 lines per segment; matrix, 220 × 256; and slice thickness, 6 mm. The inversion time (200–300 milliseconds) was adjusted to null signal from normal myocardium.

MRI Analysis

Cine MR images were analyzed to determine LV function. Using a software system (MASS, version 4.0, MEDIS Medical Imaging Systems), endocardial and epicardial borders in both end-diastolic and end-systolic phases were outlined manually on all short axes and the horizontal long axis in the cine MR images. For global LV function, the LV volume and ejection fraction were derived from all short-axis images and the horizontal long-axis images using a modified Simpson rule model [18]. The LV end-diastolic volume (LVEDV) index (LVEDV / body surface area ratio) was calculated for normalization. For assessment of regional parameters, MR images were analyzed according to a 29-segment model of the LV (Fig. 1).

Using MASS, version 4.0, we measured the regional end-diastolic wall thickness; the wall motion, indicating the extent of movement of the inner ventricular wall relative to the center of the cavity between the end-diastolic and end-systolic phases; and the wall thickening, indicating the increased rate (percentage) of wall thickness between the end-systolic and end-diastolic phases. We analyzed the relationship of the regional myocardial function results to the regional myocardial hyperenhancement.

Regional hyperenhancement was scored by consensus of two radiologists based on the proportion of hyperenhanced myocardial area to the total segmental area (0 = no hyperenhancement, 1 = 1–25%, 2 = 26–50%, 3 = 51–75%, and 4 = 76–100% hyperenhancement). First, the hyperenhancement scores for each short axis slice and

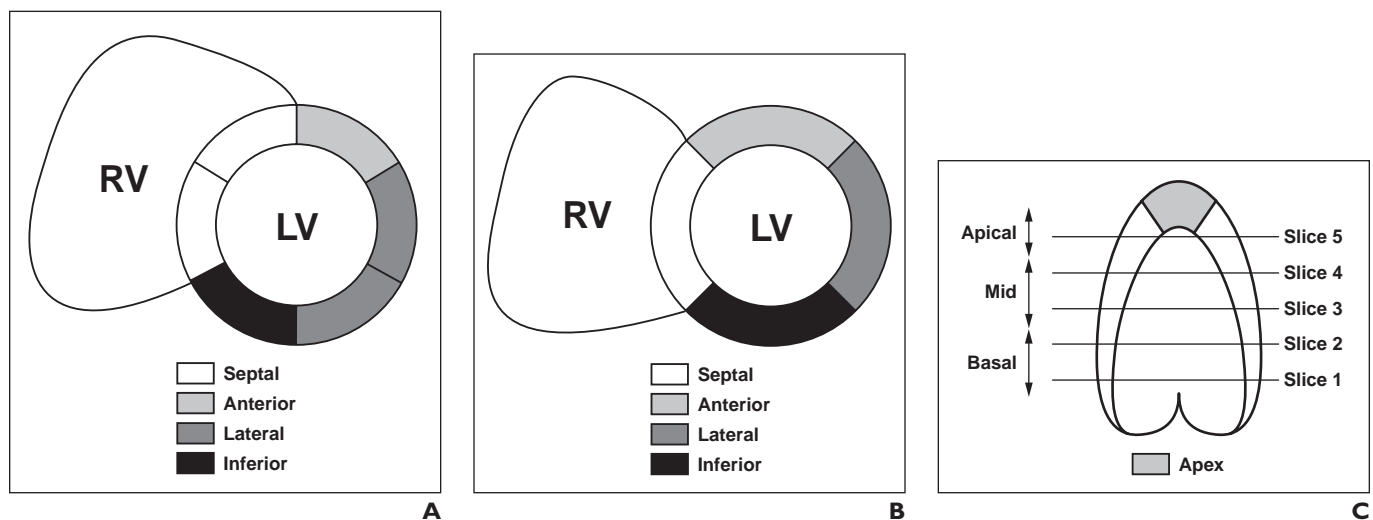


Fig. 1—29-segment model of left ventricle.

A–C, Diagrams illustrate basal and mid short-axis slices (**A**), apical short-axis slice (**B**), and horizontal long-axis slice (**C**). In diagrams that correspond to basal slices 1 and 2 (**A**) and mid slices 3 and 4 (**C**), left ventricular (LV) myocardium is divided into six segments including anterior, lateral, inferior, and septal walls, whereas it is divided into four segments in slice 5 of diagram (**B**), which corresponds to apical slice 5 in diagram (**C**). LV myocardium at extreme tip of ventricle apex (gray shading, **C**), where there is no longer cavity, is defined as another segment, apex. RV = right ventricle.

TABLE 1: Clinical Characteristics of the Patients With and Those Without Cardiac Sarcoidosis

Characteristic	Patients With Cardiac Sarcoidosis (n = 11)	Patients Without Cardiac Sarcoidosis (n = 29)	p
Age (y), mean ± SD	54 ± 16	45 ± 16	NS
NYHA functional class, no. of patients			
I	5	29	
II	6	0	
III	0	0	
IV	0	0	
Period after the diagnosis of sarcoidosis (mo), mean ± SD	22 ± 33	46 ± 45	NS
Pulmonary stage (I–IV), mean ± SD	1.1 ± 0.7	1.5 ± 0.6	NS
No. (%) of patients			
Treated with steroids after MRI study	10 (91)	3 (10)	<0.00001
Palpitation	5 (45)	5 (13)	NS
Syncope	1 (9)	0 (0)	NS
Angiotensin-converting enzyme (IU/L), mean ± SD	15 ± 11	24 ± 10	<0.05
Brain natriuretic peptide (pg/mL), mean ± SD	137 ± 119	16 ± 14 ^a	<0.0001
No. (%) of patients with abnormal findings on			
12-lead ECG	11 (100)	6 (21)	<0.00001
Holter ECG	10 (91)	2 (7)	<0.005
Echocardiography	9 (82)	3 (11)	<0.00005

Note—NS = not significant, NYHA = New York Heart Association.

^aLevels were available for 22 of the 29 patients without cardiac sarcoidosis.

for each myocardial wall (septal, anterior, lateral, and inferior walls in Fig. 1) were averaged for each patient. Then, the total sum of hyperenhancement scores for all 29 segments was obtained for each patient. For example, a patient with a hyperenhancement score of 4 in all segments would have a hyperenhancement score sum of 116.

Each segment was further divided into three layers—subepicardial, midmyocardial, and subendocardial—and each layer was assessed for hyperenhancement. Partially hyperenhanced layers were deemed hyperenhanced. The patterns of hyperenhancement within each segment were defined as follows: A, no hyperenhancement; B, transmural hyperenhancement; C, subepicardial layer–dominant hyperenhancement; D, midmyocardial layer–dominant hyperenhancement; E, subendocardial layer–dominant hyperenhancement; and F, hyperenhancement of subepicardial and subendocardial layers with an intervening zone of nonenhanced midmyocardial layer. Subepicardial layer–dominant hyperenhancement was defined as hyperenhancement predominantly involving the subepicardial layer with possible

extension into the midmyocardial layer. Similarly, subendocardial layer–dominant hyperenhancement was defined as involving the subendocardial layer with possible extension into the midmyocardial layer. Midmyocardial layer–dominant hyperenhancement was defined as being confined to the midmyocardial layer. To more clearly compare the predominant hyperenhancement among the three layers, the number of hyperenhanced segments was counted for each layer per patient.

Statistical Analyses

All values are expressed as means ± SD. We used analysis of variance with repeated measures followed by a post-hoc Bonferroni test to analyze statistical differences among different myocardial regions. We used analysis of variance to analyze statistical differences among regions with different hyperenhancement scores, whereas differences between the two groups were analyzed using an unpaired Student's *t* test. We used simple linear regression analysis for correlations between the global extent of hyperenhanced myocardium and the LVEDV index, the LV ejection fraction, or the

plasma concentration of BNP. The proportion of subgroups in the nontransmural hyperenhanced group was compared using the chi-square test for goodness of fit. A *p* value of <0.05 was considered statistically significant.

Results

The clinical characteristics of the patients with and without cardiac sarcoidosis are shown in Table 1. Although the mean age of the patients with cardiac sarcoidosis was 9 years greater than that of the patients without cardiac sarcoidosis, the difference was not significant. None of the patients without cardiac sarcoidosis had previous heart failure, whereas six of the 11 patients with cardiac sarcoidosis had a history of heart failure. The markers associated with cardiac function (plasma BNP level; and abnormal findings on 12-lead ECG, 24-hour Holter ECG, or echocardiography) were significantly higher in patients with cardiac sarcoidosis than in those without cardiac sarcoidosis ($p < 0.0001$, $p < 0.00001$, $p < 0.005$, and $p < 0.00005$, respectively). Other symptoms of the 11 patients with cardiac sarcoidosis included dyspnea ($n = 4$), chest pain ($n = 2$), syncope ($n = 1$), and palpitations ($n = 5$). Two patients with cardiac sarcoidosis were asymptomatic. The representative ECG findings included atrioventricular block ($n = 6$), ST-T wave abnormality ($n = 2$), abnormal Q wave ($n = 1$), bundle branch block ($n = 1$), and premature ventricular contraction ($n = 1$). The MRI indexes in patients with cardiac sarcoidosis were the LVEDV index (mean ± SD, 102 ± 26 mL/m²), the LV ejection fraction ($42\% \pm 14\%$), and the sum of the hyperenhancement score (47 ± 22).

Representative MR images are shown in Figures 2 and 3. Ten of the 11 cardiac sarcoidosis patients showed myocardial hyperenhancement (positive in 202 of 319 segments), whereas none of the 29 patients without cardiac sarcoidosis showed hyperenhancement.

In patients with cardiac sarcoidosis, myocardial hyperenhancement was significantly more extensive in the basal-side short axis slices than in the apical-side short axis slices ($p < 0.0005$, Fig. 4A). The extent of myocardial hyperenhancement was not significantly different among the septal, anterior, lateral, and inferior walls in patients with cardiac sarcoidosis (Fig. 4B). Myocardial hyperenhancement was significantly more frequent in the subepicardial layers than in the subendocardial layers in cardiac sarcoidosis patients ($p < 0.0001$, Fig. 4C).

MRI of Cardiac Sarcoidosis

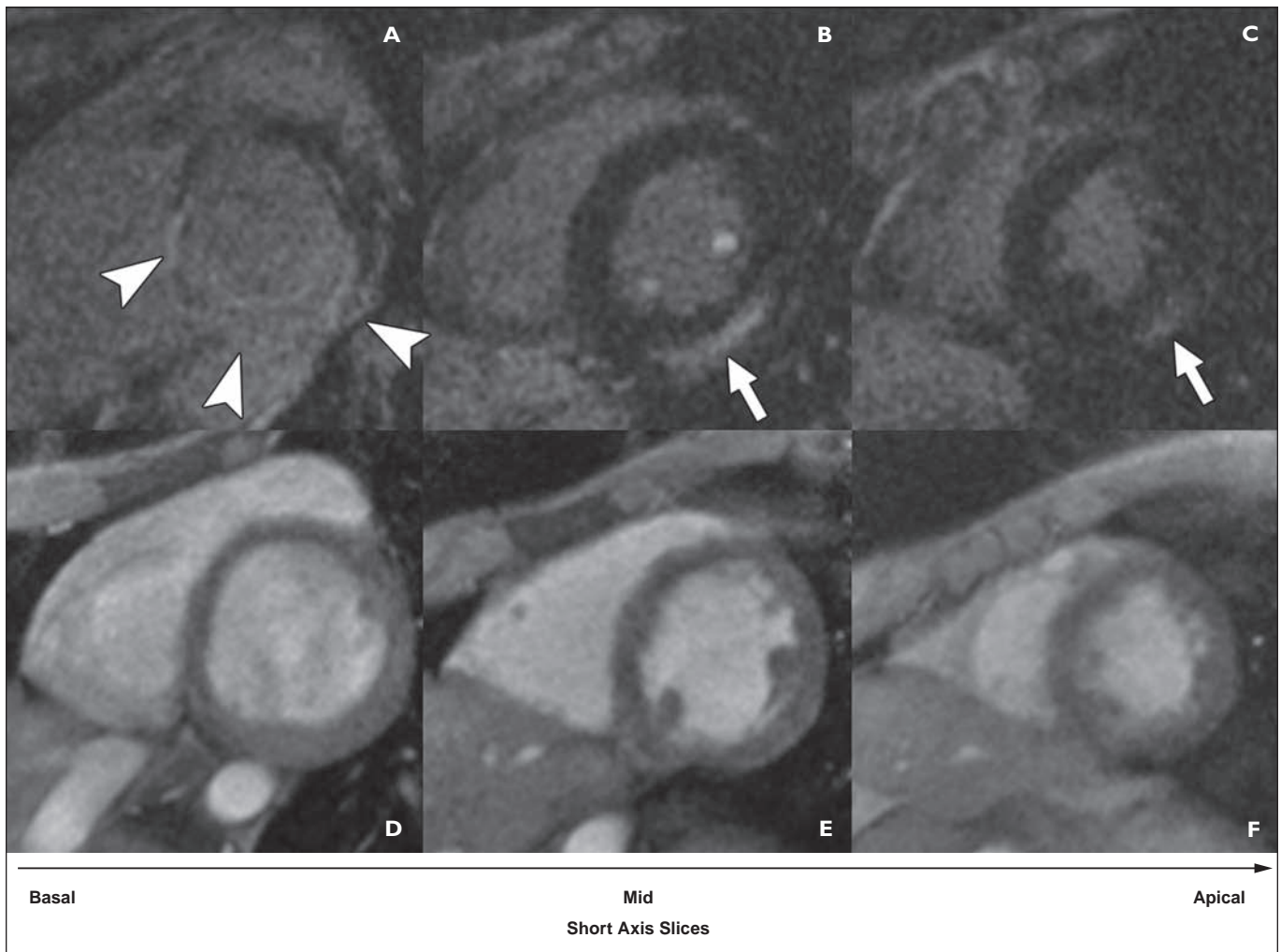


Fig. 2—27-year-old man with cardiac sarcoidosis and intact coronary arteries on coronary angiography (patient 1). Delayed contrast-enhanced MR images (A–C) and corresponding (by slice) cine MR images (D–F). Delayed contrast-enhanced MR images show apparent hyperenhancement that primarily involves basal side at interventricular septum, inferior wall, and lateral wall (arrowheads, A) and extends to inferior to lateral portions of mid slices and apical slices (arrows, B and C). Hyperenhancement is predominantly present in epicardial layer of myocardium. Wall with hyperenhancement does not show thinning and is of normal thickness on cine MR images.

In patients with cardiac sarcoidosis, 71 myocardial segments showed transmural hyperenhancement (pattern B), and 131 myocardial segments showed nontransmural hyperenhancement (patterns C–F, Table 2). Among the nontransmural patterns, subepicardial layer–dominant hyperenhancement (pattern C) was the most frequent ($p < 0.01$).

Regional wall thickening and regional wall motion were significantly reduced in the segments with a hyperenhancement score of 4 compared with segments with hyperenhancement scores of 0–3 ($p < 0.0001$, Fig. 5A and $p < 0.0001$, Fig. 5B, respectively). Regional wall thickness did not differ significantly among the segments with different scores (Fig. 5C). In patients with cardiac sarcoidosis, the sum of the hyperenhancement scores was sig-

nificantly correlated with the plasma concentration of BNP and the LVEDV index ($r = 0.75$, $p < 0.01$, and $r = 0.61$, $p < 0.05$, respectively) and was negatively correlated with the LV ejection fraction ($r = -0.76$, $p < 0.01$; Fig. 6).

Discussion

Diagnosis of Cardiac Sarcoidosis by MRI

Delayed contrast-enhanced MRI with an inversion recovery technique detects infarcted lesions with greater sensitivity and accuracy than conventional contrast spin-echo imaging [7]. Furthermore, because delayed contrast-enhanced MRI has higher spatial resolution than SPECT, it can detect small subendocardial infarcts often missed by SPECT [9]. In addition, in patients with cardiac sarcoidosis, hyperenhancement of myo-

cardial lesions has been reported [11–13, 19–21]. Recently, Smedema et al. [11] and Tadamura et al. [13] studied MR images from cardiac sarcoidosis patients; however, neither group of investigators statistically analyzed the extent or distribution of hyperenhancement in cardiac sarcoidosis using delayed contrast-enhanced MRI with an inversion recovery technique. Furthermore, we have found no studies to date that examine the association between hyperenhancement and LV global function or neurohumoral activation in cardiac sarcoidosis patients. For the first time, using delayed contrast-enhanced MRI with an inversion recovery technique, we have identified a characteristic distribution of hyperenhancement and a significant correlation between hyperenhancement and

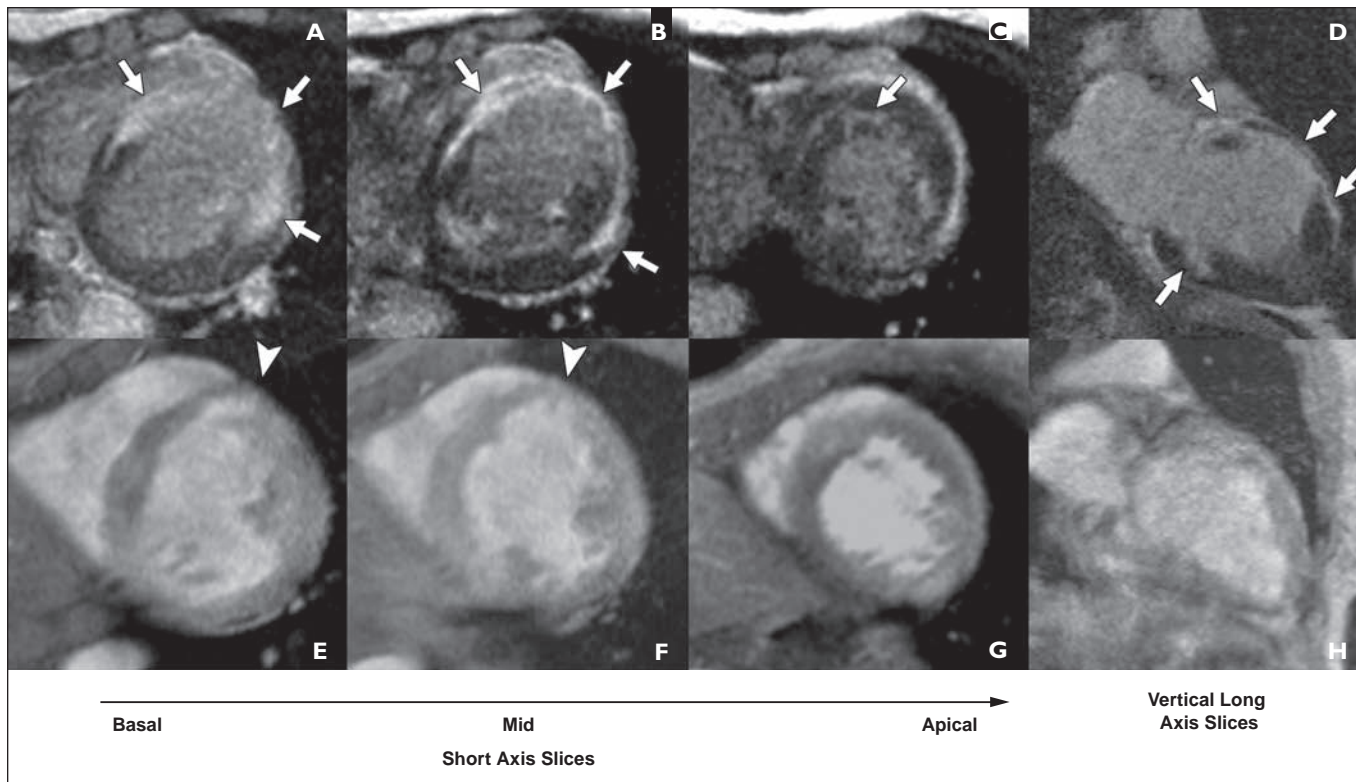


Fig. 3—76-year-old woman with cardiac sarcoidosis and intact coronary arteries on coronary angiography (patient 6). Delayed contrast-enhanced MR images (A–D) and corresponding (by slice) cine MR images (E–H). Basal mid anterior wall with hyperenhancement shows decreased thickness of myocardium (arrowheads, E and F) on cine MR images. Arrows = hyperenhancement of myocardium.

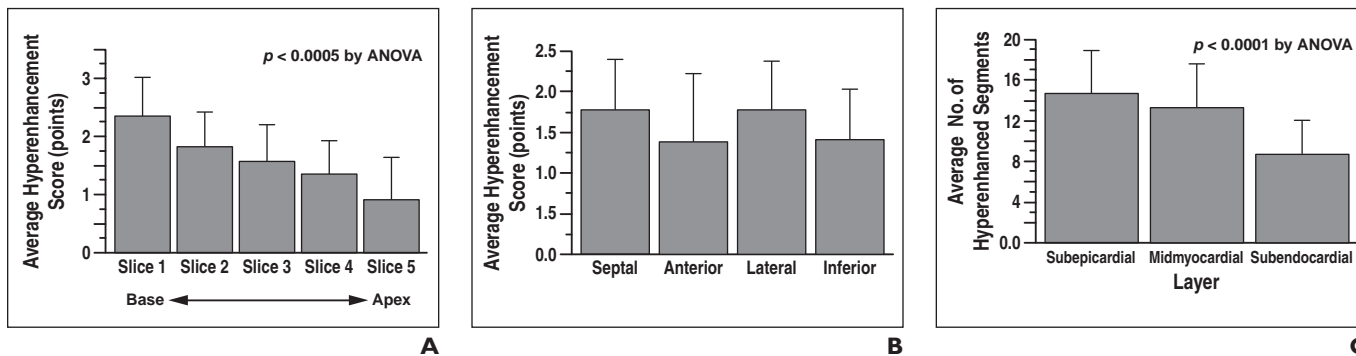


Fig. 4—Localization of myocardial hyperenhancement, which was scored as follows: 0 = no hyperenhancement, 1 = 1–25%, 2 = 26–50%, 3 = 51–75%, and 4 = 76–100% hyperenhancement. Horizontal lines (“whiskers”) above each bar show standard error. ANOVA = analysis of variance.
A, Bar graph shows average hyperenhancement score for short axis slices. For slice 1, $p < 0.05$ versus slice 4 and $p < 0.005$ versus slice 5; for slice 2, $p < 0.05$ versus slice 5.
B, Bar graph shows average hyperenhancement score for each myocardial wall.
C, Bar graph shows average number of hyperenhanced segments in subepicardial, midmyocardial, and subendocardial layers per patient. For subepicardial layer, $p < 0.05$ versus subendocardial layer.

LV global function and increased plasma BNP in patients with cardiac sarcoidosis.

Our results indicate that cardiac sarcoidosis predominantly affects the basal myocardium and the subepicardial layer. Moreover, the extent of myocardial hyperenhancement is significantly correlated with the plasma concentration of BNP and the LVEDV index and is negatively correlated with the LV ejection fraction.

The Mechanism of Myocardial Hyperenhancement in Cardiac Sarcoidosis

Delayed contrast-enhanced MRI is well established for visualizing lesions in patients with MI [7, 8]. Although the mechanism of myocardial hyperenhancement may differ between acute and chronic MI, hyperenhancement is associated with an increased volume of gadolinium chelates secondary to extracellular space expansion in acute MI

and chronic myocardial lesions [7, 8]. Mahrholdt et al. [10] reported that the region of myocardial hyperenhancement was closely related to the histopathology of active myocarditis. They hypothesized that necrotic cells, characterized by ruptured membranes, may be responsible for hyperenhancement in patients with myocarditis.

Results from several studies have shown hyperenhancement of myocardial lesions in

TABLE 2: Patterns of Myocardial Hyperenhancement in 11 Patients with Cardiac Sarcoidosis

Myocardial Enhancement Patterns	No. of Enhanced Segments
None (pattern A)	117
Transmural (pattern B)	71
Nontransmural (patterns C–F)	
Hyperenhancement patterns	
Subepicardial layer dominant (pattern C)	89
Mid myocardial layer dominant (pattern D)	17
Subendocardial layer dominant (pattern E)	21
Hyperenhancement of subepicardial and subendocardial layers (pattern F)	4
Total	319

patients with cardiac sarcoidosis [11–13, 19–21]; however, histologic evidence showing hyperenhancement has not been reported in cardiac sarcoidosis patients to date. Pathologic studies have shown that the histologic features of cardiac sarcoidosis consist of nonspecific inflammatory changes such as infiltration of lymphocytes, interstitial edema, and damaged cardiac myocytes, resulting in interstitial fibrosis or scarring [21]. We suspect myocardial hyperenhancement in cardiac sarcoidosis may share common histologic features with myocardial hyperenhancement in MI and myocarditis (i.e., scars and inflammatory changes).

In the present study, we found that myocardial wall thickening and wall motion were decreased with an increase in hyperenhancement score, as has been reported in patients with MI [22, 23], whereas wall thickness was not significantly decreased in extensively enhanced myocardial segments. Scarring in cardiac sarcoidosis is known to be associated with granulomatous changes [24], being quite different from that in MI, and thus it may not necessarily result in wall thinning.

The Topographic Localization of Myocardial Hyperenhancement

In the present study, the analysis of regional myocardial hyperenhancement revealed that myocardial lesions were frequently located in the basal myocardium rather than in the apical myocardium. The localization of hyperenhancement in the basal myocardium is consistent with earlier morphologic and pathologic studies showing the basal localization of sarcoid lesions [13, 24]. Several echocardiographic studies have shown that the interventricular septum is frequently affected in sarcoidosis [5, 25]; and in a necropsy study, Roberts et al. [24] reported that the LV-free wall was the most common location. In contrast, we did not find any significant differences in the extent of hyperenhancement between the septal, anterior, lateral, and inferior walls; this result may be explained by differences in the diagnostic techniques between the two studies. Echocardiography may be limited to showing the entire LV myocardium because it is often better for depicting the interventricular septum

than the LV-free wall. This approach could lead to a disproportionate detection of abnormalities in the interventricular septum.

The Intramural Localization of Myocardial Hyperenhancement

Echocardiography is unable to detect the intramural localization of sarcoid lesions. It is also difficult to identify the intramural localization of sarcoid lesions using SPECT or PET because of their limited spatial resolution. Delayed contrast-enhanced MRI with an inversion recovery technique has good spatial resolution and a good contrast ratio between diseased and normal myocardium, making it suitable for analyzing the intramural localization of small myocardial lesions [17]. We have found, using delayed contrast-enhanced MRI, that the myocardial hyperenhancement in cardiac sarcoidosis was predominantly located transmurally or in the subepicardial layer of the LV myocardium. This relatively higher frequency of subepicardial involvement is consistent with the results of an autopsy study [4] and a recent MRI study of patients with myocarditis [10].

Although the cause of sarcoidosis is unknown, histology of sarcoid lesions shows a variety of inflammatory cells [4, 26]. We speculate that the relatively frequent localization of hyperenhancement in the subepicardial layer might represent a characteristic feature of inflammatory myocardial diseases distinct from ischemic heart disease, in which preferential hyperenhancement of the subendocardial layer has been repeatedly reported [7, 8].

Correlations Between Hyperenhancement and LV Enlargement and LV Systolic Dysfunction

In the present study, the extent of hyperenhancement was significantly correlated with

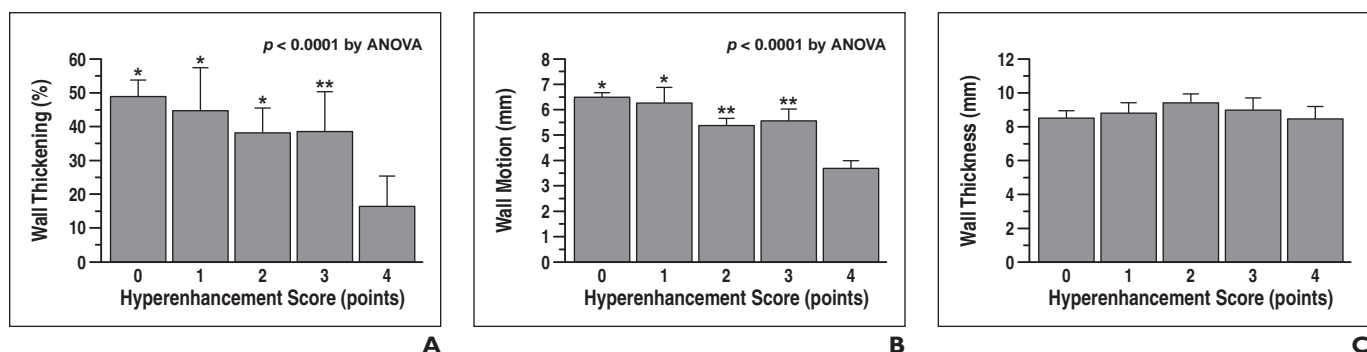


Fig. 5—Bar graphs show relationship of hyperenhancement score (0 = no hyperenhancement, 1 = 1–25%, 2 = 26–50%, 3 = 51–75%, and 4 = 76–100% hyperenhancement) to characteristics of myocardial wall. Horizontal lines (“whiskers”) above each bar show standard error.

A–C, Relationship of hyperenhancement score to regional myocardial wall thickening (**A**), wall motion (**B**), and wall thickness (**C**). Single asterisk indicates $p < 0.0001$ versus score of 4, double asterisk indicates $p < 0.005$ versus score of 4.

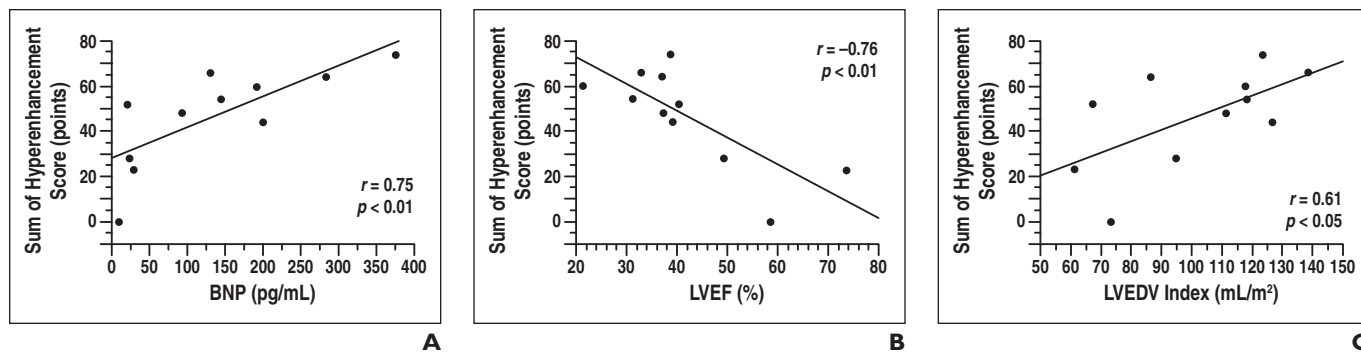


Fig. 6—Graphs show correlation between sum of hyperenhancement score (0 = no hyperenhancement, 1 = 1–25%, 2 = 26–50%, 3 = 51–75%, and 4 = 76–100% hyperenhancement) and other indicators of cardiac function.

A–C, Correlation between sum of hyperenhancement score and plasma concentration of brain natriuretic peptide (BNP) (**A**), left ventricular ejection fraction (LVEF) (**B**), and left ventricular end-diastolic volume (LVEDV) index (**C**).

the LVEDV index and was negatively correlated with the LV ejection fraction. These results may be analogous to the observation that infarct size is one of the most important determinants of LV enlargement and LV systolic dysfunction after MI [27]. The extent of hyperenhancement was positively correlated with plasma BNP level, which is correlated with the extent of ventricular dysfunction [28], development of cardiac arrhythmias [29], and long-term survival [15] in patients with heart failure. Although the mechanism of myocardial hyperenhancement in patients with cardiac sarcoidosis is not fully understood, these results suggest that the extent of hyperenhancement may be related to impaired LV function in cardiac sarcoidosis, as seen in patients after MI. In support of this theory, the plasma concentration of BNP has recently been reported to be a useful marker for identifying patients with cardiac sarcoidosis [30].

Clinical Implications

Our results suggest that delayed contrast-enhanced MRI with an inversion recovery technique is useful for diagnosing myocardial lesions in patients with cardiac sarcoidosis and that the myocardial lesions are predominantly localized in the basal and subepicardial myocardium. Localization of myocardial hyperenhancement to these regions may be a characteristic feature of cardiac sarcoidosis and may be useful for differentiating cardiac sarcoidosis from MI, which typically shows preferential hyperenhancement of the subendocardial layer [7, 8]. Although cardiac MRI is a useful tool for assessing myocardial damage and cardiac function in patients with clinically suspicious cardiac sarcoidosis, MRI is not indicated for evaluating those with sarcoidosis and no clinical signs of cardiac involvement. Because our results show

that the sum of the hyperenhancement scores significantly correlated with LV function, more extensive hyperenhancement may indicate worsened LV function in patients with cardiac sarcoidosis. The long-term prognosis of patients with and those without cardiac sarcoidosis was not evaluated in the present study and needs further study.

Study Limitations

We could not obtain histologic confirmation of myocardial sarcoid lesions in individual patients; therefore, it remains unclear whether subacute or chronic myocardial sarcoid lesions might have influenced LV function parameters and plasma levels of BNP.

Our MRI protocol did not include T2-weighted MRI, which has been shown to be useful for detecting the acute inflammatory process of myocardial sarcoidosis in patients with cardiac sarcoidosis [20]. Thus, a combination of segmented inversion recovery gradient-echo pulse sequences and T2-weighted sequences might provide increased sensitivity for detecting myocardial sarcoid lesions compared with our imaging protocol.

The relationship between the presence of heart failure in patients with cardiac sarcoidosis and the MRI findings was not assessed in this study because MRI was performed after the patients had been clinically stabilized by treatment for heart failure.

Conclusion

In patients with cardiac sarcoidosis, lesions detected by delayed contrast-enhanced MRI were predominantly localized in the basal side of the myocardium and tended to show subepicardial or transmural involvement. Hyperenhancement may be related to LV dysfunction in patients with cardiac sarcoidosis.

Acknowledgments

We are grateful to Ichiro Tsuji for his support in statistical analysis and Tatsuo Nagasaka and the other radiologic technologists for their support in performing the MRI examinations.

References

- Newman LS, Rose CS, Maier LA. Sarcoidosis. *N Engl J Med* 1997; 336:1224–1234
- Silverman KJ, Hutchins GM, Bulkley BH. Cardiac sarcoid: a clinicopathologic study of 84 unselected patients with systemic sarcoidosis. *Circulation* 1978; 58:1204–1211
- Sharma OP, Maheshwari A, Thaker K. Myocardial sarcoidosis. *Chest* 1993; 103:253–258
- Matsui Y, Iwai K, Tachibana T, et al. Clinicopathological study of fatal myocardial sarcoidosis. *Ann N Y Acad Sci* 1976; 278:455–469
- Hyodo E, Hozumi T, Takemoto Y, et al. Early detection of cardiac involvement in patients with sarcoidosis by a non-invasive method with ultrasonic tissue characterisation. *Heart* 2004; 90:1275–1280
- Kinney EL, Caldwell JW. Do thallium myocardial perfusion scan abnormalities predict survival in sarcoid patients without cardiac symptoms? *Angiology* 1990; 41:573–576
- Kim RJ, Wu E, Rafael A, et al. The use of contrast-enhanced magnetic resonance imaging to identify reversible myocardial dysfunction. *N Engl J Med* 2000; 343:1445–1453
- Wagner A, Mahrholdt H, Holly TA, et al. Contrast-enhanced MRI and routine single photon emission computed tomography (SPECT) perfusion imaging for detection of subendocardial myocardial infarcts: an imaging study. *Lancet* 2003; 361:374–379
- Choudhury L, Mahrholdt H, Wagner A, et al. Myocardial scarring in asymptomatic or mildly symptomatic patients with hypertrophic cardiomyopathy. *J Am Coll Cardiol* 2002; 40:2156–2164
- Mahrholdt H, Goedecke C, Wagner A, et al. Car-

MRI of Cardiac Sarcoidosis

- diovascular magnetic resonance assessment of human myocarditis: a comparison to histology and molecular pathology. *Circulation* 2004; 109: 1250–1258
11. Smedema JP, Snoep G, van Kroonenburgh MP, et al. Evaluation of the accuracy of gadolinium-enhanced cardiovascular magnetic resonance in the diagnosis of cardiac sarcoidosis. *J Am Coll Cardiol* 2005; 45:1683–1690
 12. Vignaux O. Cardiac sarcoidosis: spectrum of MRI features. *AJR* 2005; 184:249–254
 13. Tadamura E, Yamamuro M, Kubo S, et al. Effectiveness of delayed enhanced MRI for identification of cardiac sarcoidosis: comparison with radionuclide imaging. *AJR* 2005; 185:110–115
 14. Rihal CS, Nishimura RA, Hatle LK, et al. Systolic and diastolic dysfunction in patients with clinical diagnosis of dilated cardiomyopathy: relation to symptoms and prognosis. *Circulation* 1994; 90: 2772–2779
 15. Tsutamoto T, Wada A, Maeda K, et al. Attenuation of compensation of endogenous cardiac natriuretic peptide system in chronic heart failure: prognostic role of plasma brain natriuretic peptide concentration in patients with chronic symptomatic left ventricular dysfunction. *Circulation* 1997; 96:509–516
 16. Hiraga H, Yuwai K, Hiroe M, et al. *Guideline for the diagnosis of cardiac sarcoidosis: study report on diffuse pulmonary diseases* [in Japanese]. Tokyo, Japan: The Japanese Ministry of Health and Welfare, 1993:23–24
 17. Simonetti OP, Kim RJ, Fieno DS, et al. An improved MR imaging technique for the visualization of myocardial infarction. *Radiology* 2001; 218:215–223
 18. Dulce MC, Mostbeck GH, Friese KK, et al. Quantification of the left ventricular volumes and function with cine MR imaging: comparison of geometric models with three-dimensional data. *Radiology* 1993; 188:371–376
 19. Shimada T, Shimada K, Sakane T, et al. Diagnosis of cardiac sarcoidosis and evaluation of the effects of steroid therapy by gadolinium-DTPA-enhanced magnetic resonance imaging. *Am J Med* 2001; 110:520–527
 20. Vignaux O, Dhote R, Duboc D, et al. Detection of myocardial involvement in patients with sarcoidosis applying T2-weighted, contrast-enhanced, and cine magnetic resonance imaging: initial results of a prospective study. *J Comput Assist Tomogr* 2002; 26:762–767
 21. Vignaux O, Dhote R, Duboc D, et al. Clinical significance of myocardial magnetic resonance abnormalities in patients with sarcoidosis: a 1-year follow-up study. *Chest* 2002; 122:1895–1901
 22. Kim RJ, Fieno DS, Parrish TB, et al. Relationship of MRI delayed contrast enhancement to irreversible injury, infarct age, and contractile function. *Circulation* 1999; 100:1992–2002
 23. Amano Y, Takayama M, Takahama K, et al. Delayed hyper-enhancement of myocardium in hypertrophic cardiomyopathy with asymmetrical septal hypertrophy: comparison with global and regional cardiac MR imaging appearances. *J Magn Reson Imaging* 2004; 20:595–600
 24. Roberts WC, McAllister HA Jr, Ferrans VJ. Sarcoidosis of the heart: a clinicopathologic study of 35 necropsy patients (group 1) and review of 78 previously described necropsy patients (group 11). *Am J Med* 1977; 63:86–108
 25. Lewin RF, Mor R, Spitzer S, et al. Echocardiographic evaluation of patients with systemic sarcoidosis. *Am Heart J* 1985; 110:116–122
 26. Sekiguchi M, Yazaki Y, Isobe M, et al. Cardiac sarcoidosis: diagnostic, prognostic, and therapeutic considerations. *Cardiovasc Drugs Ther* 1996; 10:495–510
 27. Pfeffer MA, Braunwald E. Ventricular remodeling after myocardial infarction: experimental observations and clinical implications. *Circulation* 1990; 81:1161–1172
 28. Yamamoto K, Burnett JC Jr, Jougasaki M, et al. Superiority of brain natriuretic peptide as a hormonal marker of ventricular systolic and diastolic dysfunction and ventricular hypertrophy. *Hypertension* 1996; 28:988–994
 29. Berger R, Huelsman M, Strecker K, et al. B-type natriuretic peptide predicts sudden death in patients with chronic heart failure. *Circulation* 2002; 105:2392–2397
 30. Yasutake H, Seino Y, Kashiwagi M, et al. Detection of cardiac sarcoidosis using cardiac markers and myocardial integrated backscatter. *Int J Cardiol* 2005; 102:259–268

APPENDIX 1: Diagnosis of Cardiac Sarcoidosis According to the Japanese Ministry of Health and Welfare Guidelines [16]

Histologic diagnosis group

Cardiac sarcoidosis is diagnosed when histologic analysis of operative or endomyocardial biopsy specimens shows epithelioid granuloma without caseating granuloma.

Clinical diagnosis group

In patients with a histologic diagnosis of extracardiac sarcoidosis, cardiac sarcoidosis is diagnosed when item (a) and one or more items (b–e) are present:

- (a) Complete right bundle branch block, left-axis deviation, atrioventricular block, ventricular tachycardia, premature ventricular contraction (> grade 2 in Lown's classification), or abnormal Q or ST-T change on ECG or Holter ECG
- (b) Abnormal wall motion, regional wall thinning or thickening, or dilatation of left ventricle on echocardiography
- (c) Perfusion defect seen on ²⁰¹Tl myocardial scintigram or abnormal accumulation of radioisotope in ⁶⁷Ga citrate or ^{99m}Tc pyrophosphate myocardial scintigraphy
- (d) Abnormal intracardiac pressure, low cardiac output, or abnormal wall motion or depressed ejection fraction of left ventricle
- (e) Interstitial fibrosis or cellular infiltration over moderate grade in endomyocardial biopsy even if findings are nonspecific